Reaction of Carbon Monoxide with the Reduced Active Site of Bacterial Nitric Oxide Reductase†

Janneke H. M. Hendriks,‡,§ Louise Prior,∥ Adam R. Baker,⊥ Andrew J. Thomson,∥ Matti Saraste,‡,▽ and Nicholas J. Watmough*,⊥

European Molecular Biology Laboratory, Meyerhofstrasse 1 D-69126 Heidelberg, Germany, Centre for Metalloprotein Spectroscopy and Biology, School of Biological Sciences, and School of Chemical Sciences, University of East Anglia, Norfolk, NR4 7TJ, United Kingdom

Received July 9, 2001; Revised Manuscript Received August 30, 2001

ABSTRACT: Bacterial nitric oxide reductase (NOR), a member of the superfamily of heme-copper oxidases, catalyzes the two-electron reduction of nitric oxide to nitrous oxide. The key feature that distinguishes NOR from the typical heme-copper oxidases is the elemental composition of the dinuclear center, which contains non-heme iron (Fe_B) rather than copper (Cu_B). UV−vis electronic absorption and room-temperature magnetic circular dichroism (RT-MCD) spectroscopies showed that CO binds to Fe(II) heme b_3 to yield a low-spin six-coordinate species. Photolysis of the Fe(II)-CO bond is followed by CO recombination ($k_{on} = 1.7 \times 10^8$ M^{-1} s^{-1}) that is approximately 3 orders of magnitude faster than CO recombination to the active site of typical heme-copper oxidases ($k_{on} = 7 \times 10^4$ M^{-1} s^{-1}). This rapid rate of CO recombination suggests an unimpeded pathway to the active site that may account for the enzyme's high affinity for substrate, essential for maintaining denitrification at low concentrations of NO. In contrast, the initial binding of CO to reduced heme b_3 measured by stopped-flow spectroscopy is much slower ($k_{on} = 1.2 \times 10^5$ M^{-1} s^{-1}). This suggests that an existing heme distal ligand (water/OH^-) may be displaced to elicit the spin-state change observed in the RT-MCD spectrum.

Nitric oxide reductase (NOR),[1] an enzyme of bacterial denitrification (*1*, *2*), is also a member of the superfamily of respiratory heme-copper oxidases (*3*, *4*). Most members of this superfamily, including the intensely studied mitochondrial cytochrome *c* oxidase (C*c*O) catalyze the four-electron reduction of dioxygen to water, a reaction that takes place at a special dinuclear site formed by high-spin heme and a copper ion Cu_B. The active site of NOR which catalyzes the two-electron reduction of NO to N_2O is also a dinuclear center, but one in which high-spin heme b_3[2] is coupled to non-heme iron (Fe_B) rather than copper (*5*, *6*).

The interaction of CO with reduced heme iron has been used to investigate the nature of the heme distal pocket in a number of oxygen-binding heme proteins including myoglobins (*7*) and heme-copper oxidases. The Fe(II)−CO bond is photolabile. The rate of recombination of photolyzed CO to the heme iron is influenced by a number of factors. These include the effective pK_a of the proximal ligand to the heme (*8*−*10*), the polarity of the heme distal pocket, and steric factors (*7*). For example, the bimolecular rate constant of recombination of CO to myoglobins that lack water in the heme distal pocket is about 50-fold faster than that to wild-type myoglobin (4×10^5 M^{-1} s^{-1}) (*7*).

The rate of recombination of CO to the active site heme of reduced heme-copper oxidases (7×10^4 $M^{-1}s^{-1}$) is considerably slower than that in the case for myoglobin (*11*, *12*). Moreover, the rate of recombination in the mitochondrial cytochrome *c* oxidase (*13*) and cytochrome bo_3 from *E. coli* (*14*) reaches a limit at CO concentrations in excess of 10 mM. These saturation kinetics can be explained in terms of a two-step mechanism in which Cu_B(I)−CO is an intermediate. The existence of this intermediate species has been demonstrated by low-temperature FTIR spectroscopy, before and after photolysis. Illumination causes a change in the CO stretching frequency from ∼1960 to ∼2050 cm^{-1} (*6*, *15*).

† Supported by grants from the UK BBSRC (83/C10160 and 83/B11958), the Commission of the European Communities (BIO4-CT98-0507), and the Wellcome Trust (054798/Z/98/Z).

* To whom correspondence should be addressed. Phone: +44 (1603) 592179. Fax: +44 (1603) 592250. E-mail: n.watmough@uea.ac.uk.

‡ European Molecular Biology Laboratory.

§ Present address: Max Planck Institute of Molecular Plant Physiology, Am Mühlenberg 1, 14476 Golm, Germany.

∥ School of Chemical Sciences.

⊥ School of Biological Sciences.

▽ Deceased May 21, 2001.

[1] Abbreviations: C*c*O, cytochrome *c* oxidase; CO, carbon monoxide; CT band, charge-transfer band; DM, dodecyl-*β*-D-maltoside; FTIR, Fourier transform infrared; k_{obs}, observed rate constant; k_{on}, bimolecular association rate constant; NO, nitric oxide; NOR, NO reductase; RT-MCD, room temperature-magnetic circular dichroism; *P. denitrificans*, *Paracoccus denitrificans*; *P. halodenitrificans*, *Paracoccus halodenitrificans*; PMS, phenazine methosulfate.

[2] The Metal Centers of NOR. To aid comparison with the heme-copper oxidases, we have adopted the following notation for the metal centers in NorB which is structurally related to C*c*O subunit I. Heme *b* is the low-spin bis-histidine coordinated heme in NorB that is a homologue of heme *a* in C*c*O. Heme b_3 is high-spin in NorB and equivalent to heme a_3 in C*c*O and heme o_3 of *E. coli* cytochrome bo_3 quinol oxidase. In C*c*O and quinol oxidases, this heme is magnetically coupled to a copper ion (Cu_B) to form a dinuclear center which is the site of oxygen binding and reduction. Fe_B is a non-heme iron in NorB, which is probably ligated by three conserved histidine residues, which serve as ligands to Cu_B in C*c*O. A fourth metal center, heme *c* is a covalently bound low-spin heme in NorC with histidine and methionine axial ligands. This site has no structural counterpart in C*c*O, but is functionally equivalent to Cu_A in that it serves as a site of electron input for the respiratory complex.

10.1021/bi011428t CCC: $20.00
Published on Web 10/13/2001

The higher frequency characteristic of Cu(I)−CO complexes is not found in oxidases lacking Cu_B ligands (*16*). Forms of bacterial heme-copper oxidases in which Cu_B is absent may be obtained by protein engineering (*14*, *17*) or by manipulating the cell culture conditions (*18*). Alternatively, Cu_B can be removed chemically by prolonged incubation of the reduced wild-type enzyme with CO (*19*). In copper-deficient oxidases, the rate of CO-binding and recombination is higher [typically $(2-4) \times 10^5$ M^{-1} s^{-1}] and proportional to the concentration of CO over the range of 0−20 mM (*14*). Thus, Cu_B serves as a transient binding site for incoming ligands, reducing the rate of binding of CO and favoring the rapid binding of dioxygen ($k_{on} \approx 1 \times 10^8$ M^{-1} s^{-1}) (*20*, *21*).

CO can bind to Fe(II) heme b_3 of NOR (*22*, *23*) to yield a complex that has been characterized by resonance Raman spectroscopy (*24*). Low-temperature FTIR spectroscopy of NOR suggests that, upon photolysis from Fe(II) heme b_3, CO can interact with Fe_B(II) (*6*). However, it is unclear whether this interaction influences the kinetics of the subsequent recombination of CO to heme b_3. Experiments designed to address this issue might also give some insights into both the organization of the active site including the chemical nature of any heme distal ligand and the pathway taken by the substrate (NO) to the active site.

Here we report an extended study of the interaction of CO with the dinuclear center of fully reduced NOR from *P. denitrificans*. The ligand binds to Fe(II) heme b_3 to form a stable complex that we have characterized by both UV−vis electronic absorption and RT-MCD spectroscopies. The rate of formation of the CO complex was 3 orders of magnitude slower than the rate of CO recombination measured by flash photolysis. These data suggest not only a rather different organization of the active site than is found in other members of the heme-copper oxidase superfamily but also that the initial binding of CO to reduced heme b_3 may require the displacement of an existing distal ligand.

MATERIALS AND METHODS

Cell Growth and Enzyme Purification. P. denitrificans strain Pd 27.21 (*ccoNO*::Km^R) (*25*) was grown in a 120 L fermentor on minimal medium under anaerobic denitrifying conditions, and the two-subunit form of the enzyme was purified as previously described (*6*). It was >99% pure as judged by polyacrylamide gel electrophoresis in the presence of sodium dodecyl sulfate and by the A_{410}:A_{280} ratio of the oxidized enzyme of 1.2.

Spectroscopy. UV−vis electronic absorbance spectra were recorded on a Hitachi U3000 spectrophotometer. Room-temperature magnetic circular dichroism (RT-MCD) spectra were recorded on a Jasco J-500D circular dichrograph. An Oxford Instruments superconducting solenoid with a 25 mm room-temperature bore was used to generate magnetic fields of up to 6 T. MCD spectral intensities depend linearly on the magnetic field at room temperature and are expressed per unit magnetic field as $\Delta\epsilon$/H (M^{-1} cm^{-1} T^{-1}) (*26*). The concentration of NOR was calculated using $\epsilon_{411} = 3.11 \times 10^5$ M^{-1} cm^{-1} (*5*). Spectra were exported as ASCII files and replotted in Axum v6.0 (MathSoft Inc).

Kinetic Measurements. The rate of recombination of CO with the reduced binuclear center was measured using an LKS.50 laser kinetic spectrophotometer (Applied Photophysics, Leatherhead, U.K.). Photolysis was initiated by a pulse of laser light (6 ns, 100 mJ, 532 nm) provided by a SL282G Nd:YAG laser equipped with frequency doubling optics (Spectron Laser Systems, Rugby, U.K.). Subsequent absorption changes at a single wavelength were recorded using a Hewlett-Packard 54520A digitizing oscilloscope.

The reaction of fully reduced NOR with CO under pseudo-first-order conditions was measured in an Applied Photophysics Bio-Sequential DX.17MV stopped-flow spectrophotometer using a 1 cm path length cell. Detection at a single wavelength was with a side window photomultiplier. Buffers containing decreasing amounts of CO were made by serial dilution with anaerobic buffer of an initially CO-saturated solution. In this configuration, a minimum of 1000 data points were collected per experiment with a split time base with a maximal time resolution of 0.2 ms. A minimum of four traces were collected at each concentration of CO.

All experiments were performed at room temperature. Experimental traces were exported as ASCII files and analyzed using either TableCurve 2D for Windows (Jandel Scientific, San Rafael, CA) or Graphit v3.0 (Erithicus Software) as a single or the sum of exponentials.

RESULTS

Electronic Absorption Spectroscopy. The electronic absorption spectrum of NOR prior to reduction was similar to that previously reported with a Soret maximum at 411 nm and broad peaks in the visible region between 530 and 560 nm (see Figure 1A). The distinct shoulder at 595 nm, which disappears upon reduction, has been assigned to a ligand−metal CT band arising from hydroxide bound to the active site high-spin heme b_3 (*5*, *27*). This band transiently shifted to 610 nm during reduction with ascorbate and phenazine methosulfate (ascorbate/PMS). A similar observation has been made during mediated redox titrations over a range of reduction potentials between +200 and +100 mV that cause full reduction of the active site non-heme iron Fe_B, but at which heme b_3 remains oxidized (*27*).

Upon reduction by ascorbate/PMS, the Soret maximum shifts to 420 nm and intensifies ($\epsilon \approx 360$ mM^{-1} cm^{-1}). In addition, two well-defined peaks appeared in the visible region at 521 and 551 nm indicating the presence of reduced low-spin heme *c*. The feature at 551 nm had a distinct shoulder at 560 nm, which is typical for low-spin Fe(II) heme *b*. The effect of adding 1 mM CO is readily seen in the electronic absorption spectrum (Figure 1A). The Soret band both narrows and intensifies ($\epsilon \approx 480$ mM^{-1} cm^{-1}) in response to CO binding, but does not shift in wavelength. These changes are apparent in the reduced-CO *minus* reduced difference spectra (Figure 1B). Note that, whatever the method of initial reduction, the amplitude of the peak in the Soret region of the reduced-CO *minus* reduced difference spectra is much larger than the amplitude of the trough centered at ~430 nm. Thus, the spectral changes that reduced NOR exhibits in response to CO binding, clearly differ from those of globins and the copper-containing heme-copper oxidases. In these proteins, CO binds to the distal face of the oxygen-binding ferrous heme, causing a spin-state change in the heme iron. This spin-state change results in a blue-shift in the Soret maximum that gives rise to a characteristic derivative-shaped difference spectrum (reduced-CO *minus*

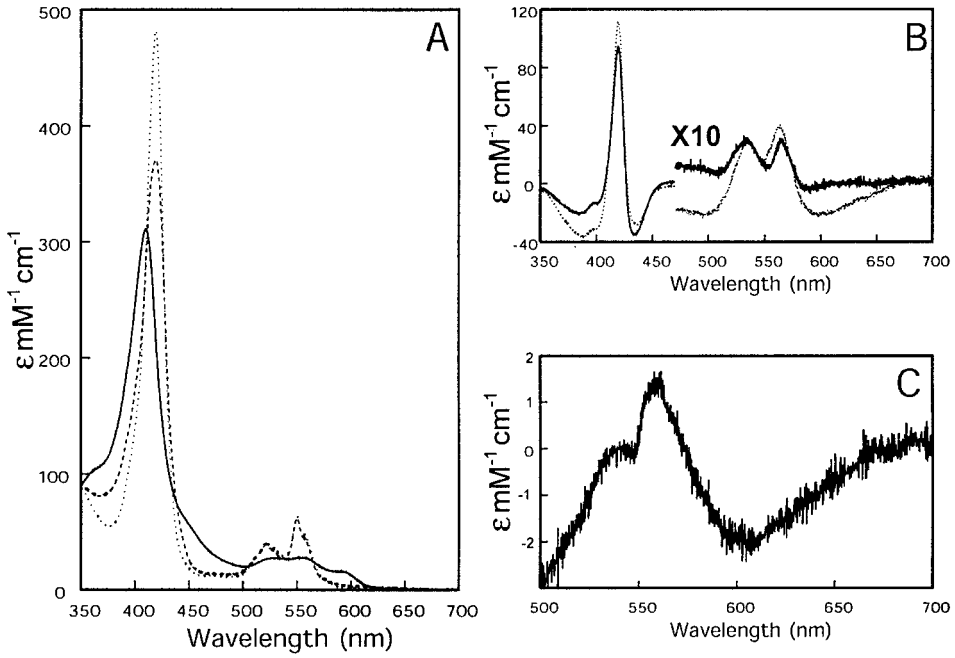

FIGURE 1: Effect of CO on the UV−vis electronic absorption spectrum of reduced NOR. Panel A shows the spectrum of 2.8 μM NOR in 50 mM potassium phosphate, 0.1 mM EDTA, 0.01% (w/v) DM, pH 8.0, in the fully oxidized state (—), after reduction by ascorbate/PMS (---), and after addition of CO (···). All solutions were equilibrated under an atmosphere of nitrogen and additions were made anaerobically. Panel B shows of the sample shown in panel A (···) and the reduced-CO *minus* reduced difference spectrum of an identical sample where after the initial reduction by ascorbate/PMS a trace of dithionite was added (—). Panel C shows the difference spectrum of the two traces of Panel B shown ([reduced-CO *minus* PMS/ascorbate reduced] *minus* [reduced-CO *minus* dithionite reduced]).

reduced) caused by the increase in absorbance in parallel with an absorbance loss of similar amplitude at adjacent higher wavelengths (see Figure 3A). The associated changes seen in the alpha band region spectrum of NOR, in response to CO binding, are similar to other hemoproteins, although less intense (Figure 1B).

When a small amount of dithionite was added to the sample prior to the addition of CO to ensure complete reduction of the high-spin heme b_3, a slightly different reduced-CO *minus* reduced visible region difference spectrum was obtained (Figure 1B). This effect of complete reduction of heme b_3 prior to the addition of CO is most clearly illustrated in the double difference ([reduced-CO *minus* PMS/ascorbate reduced] *minus* [reduced-CO *minus* dithionite reduced]) spectrum (Figure 1C).

Room-Temperature MCD Spectroscopy of Reduced NOR. One explanation for the unusual static electronic absorption difference spectrum could be that, in at least a fraction of the fully reduced enzyme, Fe(II) heme b_3 already has a distal ligand, possibly exogenous, and is therefore already low-spin. Consequently, CO must displace this ligand to yield a six-coordinate Fe(II)−CO species, as happens in the cases of CooA from *Rhodospirillum rubrum* (*28*) and soluble guanylyl cyclase (*29*). Changes in heme ligation state are readily observed by RT-MCD spectroscopy (*28*, *29*), as is the high- to low-spin transition that accompanies the binding of CO to Fe(II) deoxymyoglobin (*30*, *31*). Therefore to determine the spin- and ligation-states of Fe(II) heme b_3 in NOR prior to CO binding, we measured the RT-MCD of samples of enzyme reduced by ascorbate/PMS (Figure 2A; solid line) and by dithionite (Figure 2A; dashed line).

The sample reduced by PMS/ascorbate contains a mixture of fully reduced and three-electron reduced NOR in a ratio of approximately 5:1 as determined by electronic absorption spectroscopy (see above and discussion). Consequently, in addition to the positive feature at 440 nm which is due to the presence of some *high-spin* Fe(II) heme b_3, the RT-MCD spectrum also contains a broad derivative shaped feature with a maximum at ~400 nm and a minimum at ~430 nm (Figure 2A; solid line). We have previously reported that this second feature dominates the RT-MCD spectrum of the three-electron reduced form of NOR (*27*).

In the dithionite reduced sample, which contains enzyme in which all the hemes are fully reduced, this broad derivative is absent and the feature at 440 nm is more prominent. Moreover, there is a new feature at ~590 nm (Figure 2A; dashed line) that may be associated with the presence of high-spin ferrous heme. However, the intensity of the 440 nm band ($\Delta\epsilon/H = 40$ M^{-1} cm^{-1} T^{-1}) would only account for approximately 50% of Fe(II) heme b_3 being in the *high-spin* state, the remainder we presume is *low-spin*.

In both PMS/ascorbate and dithionite reduced samples, there is little of the intensity in the Soret region of the RT-MCD spectrum that would normally be associated with the presence of multiple low-spin ferrous hemes. This is probably a result of three overlapping MCD A-terms with different zero-crossover points, corresponding to the absorbance maxima of Fe(II) heme *c*, Fe(II) heme *b*, and any *low-spin* Fe(II) heme b_3. The consequences of the overlap of such derivatives are even more obvious in the visible region of the RT-MCD spectrum. Here reduced heme *b* and *c* contribute to a complex feature with a maximum at 540 nm and minima at 550 and 560 nm. The apparent intensity of these features in the visible region is governed by the underlying spectrum of heme b_3. In the PMS/ascorbate reduced sample (Figure 2A; solid line) this is a mixture of ferrous and ferric forms and in the dithionite reduced sample

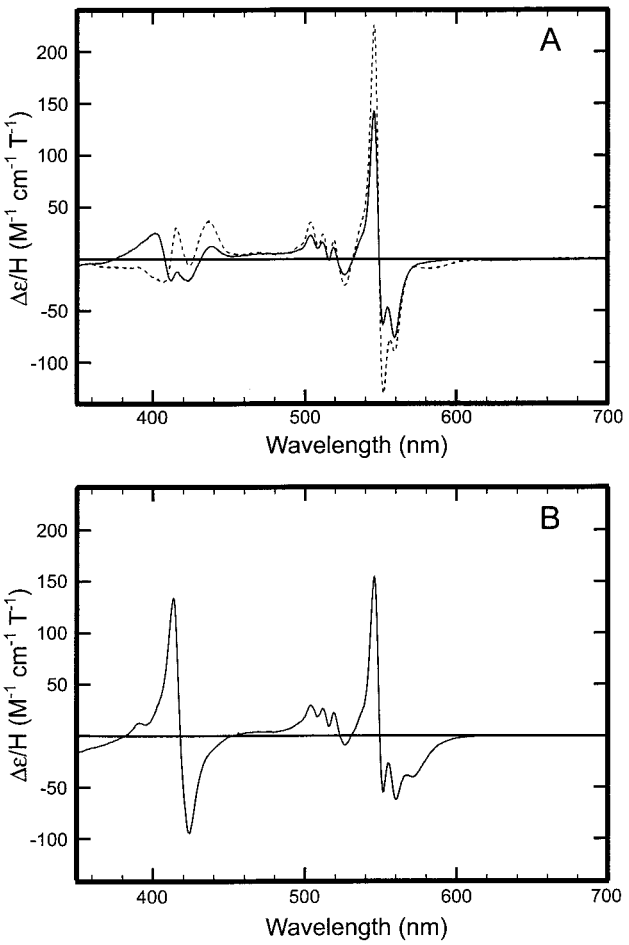

FIGURE 2: RT-MCD spectrum of reduced NOR in the presence and absence of 1 mM CO. Samples of NOR (~60 μM) were prepared as described in the legend to Figure 1A and reduced with ascorbate/PMS (—) or with dithionite (---) (A). Panel B shows the effect of treating the sample reduced with dithionite shown in panel A with 1 mM CO.

(Figure 2A; dashed line), all ferrous, but a mixture of high- and low-spin species.

The RT-MCD spectrum of reduced NOR after exposure to 1 mM CO is shown in Figure 2B and resembles that of the reduced NOR of *P. halodenitrificans* in the presence of CO (*32*). In fact, the spectrum of the reduced NOR−CO complex is the same irrespective of the method used to initially reduce the enzyme. This indicates that in the case of PMS/ascorbate reduced NOR the subsequent addition of CO leads to complete reduction of the active site. This could be for one of two reasons. Either the CO is acting as a reductant, or alternatively the binding of CO to the population of heme b_3 that is already reduced traps the electron there, thus shifting the Fe(II)/Fe(III) equilibrium toward complete reduction of heme b_3.

The Soret region of the RT-MCD spectrum of the reduced NOR−CO complex (Figure 4B) resembles that of a number of other ferrous heme proteins with histidine/CO axial coordination. These include myoglobin (*30, 31*), soluble guanylyl cyclase (*29*), and CooA (*28*). Superficially, the complex feature in the visible region of the spectrum resembles that seen in fully (dithionite) reduced NOR (Figure 4A; dashed line). However, there is now a new minimum at 572 nm, which corresponds to a loss of intensity in the region 550−570 nm (Figure 2B). The new minimum is the negative

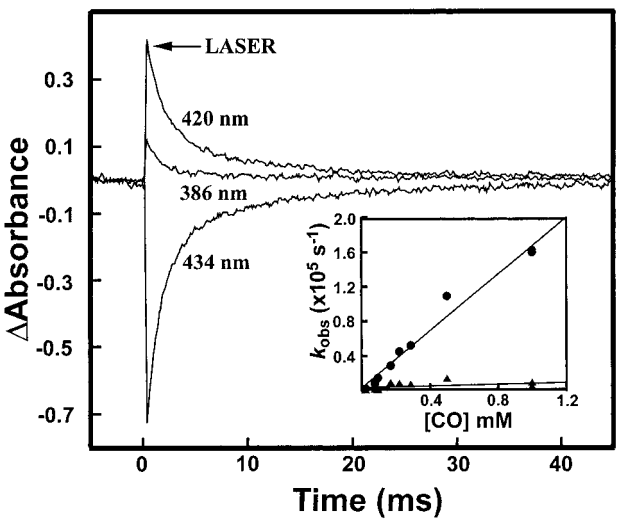

FIGURE 3: Recombination of CO to reduced NOR after flash photolysis. The spectral changes over time recorded at 386, 420, and 434 nm that are induced by photolysis of the reduced NOR-CO (prepared as described in the legend to Figure 1) in the presence of 1 mM CO, The inset shows the observed rates (k_{obs}) of the fast (●) and slow (▲) phases of CO recombination to reduced NOR monitored at 419 nm plotted as a function of CO concentration.

lobe of an MCD A-term that has been observed in the CO derivatives of other Fe(II) heme proteins (*28*−*31*). This derivative has a corresponding positive lobe at ~560 nm, which would account for the loss of intensity in that region. Thus, the RT-MCD spectrum of the CO derivative of reduced NOR is consistent with all of the heme b_3 being low-spin ferrous when CO is the distal ligand.

Laser Flash Photolysis. The electronic absorption difference spectrum (reduced *minus* reduced-CO) of high-spin Fe(II) heme b_3 can also be obtained from the initial absorbance change induced by photolysis of the CO at various wavelengths. The difference spectrum after photolysis would be expected to be the inverse of the static difference spectrum, unless the enzyme formed transiently after photolysis is spectroscopically different from the initially reduced enzyme.

The rate of recombination of CO with Fe(II) heme b_3 after photolysis was initially monitored at 419 nm, the point of maximum change in the static difference spectrum. The amplitude of the absorbance change associated with CO recombination was dependent on the wavelength used to monitor the reaction (Figure 3). Recombination was observed to be biphasic with a dominant fast phase, accounting for ca. 75% of the absorbance change. In the presence of 1 mM CO, the rate of recombination (k_{obs}) of the fast phase was $\sim 2 \times 10^5$ s^{-1}. The recombination rates of both phases showed a linear dependence on the CO concentration (Figure 3 insert). Thus, recombination is not geminate, and the bond between the Fe(II) heme b_3 and CO is completely broken upon photolysis. The bimolecular rate constant of the fast phase ($k_{on} = 1.7 \times 10^8$ M^{-1} s^{-1}) is the fastest recorded CO recombination to a ferrous hemoprotein (Table 1).

Recombination was monitored at a series of wavelengths between 380 and 450 nm at intervals of 2.5 nm and the photolysis difference spectrum (reduced *minus* reduced-CO) was calculated. The geometry of the flash-photolysis apparatus is such that the laser pulse does not pass through the whole sample and as a consequence not all the Fe(II)−

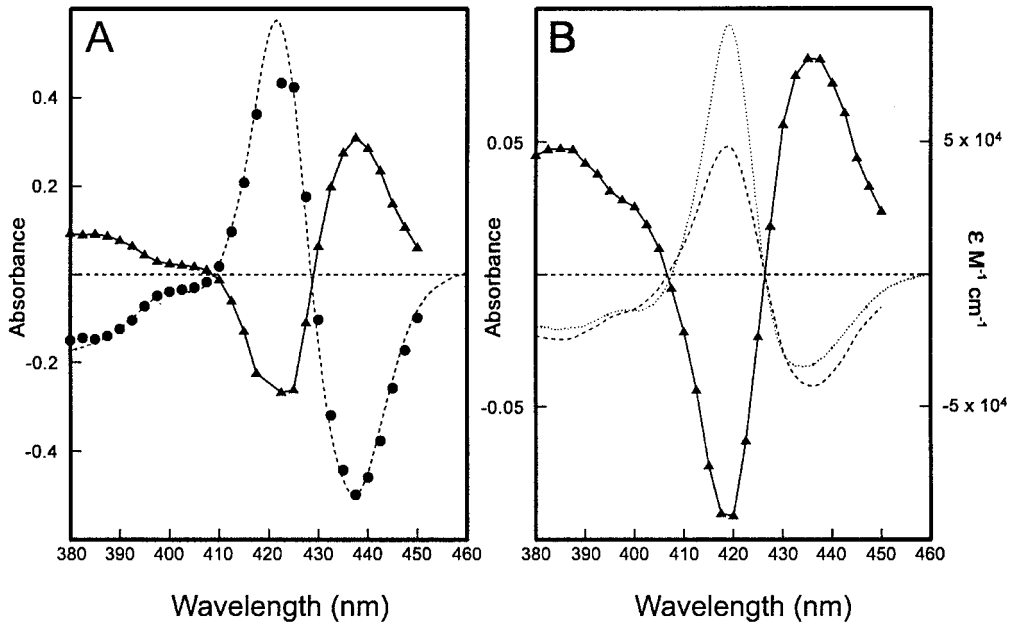

FIGURE 4: Comparison of the kinetic and static CO difference spectra of NOR. Panel A shows the Soret region of the static reduced-CO *minus* reduced spectrum of 10 μM horse heart myoglobin in 50 mM potassium phosphate pH 8.0 (---). The post photolysis (0.2 μs), (▲) was calculated at 2.5 nm intervals. Since the entire population Fe(II) carbonmonoxymyoglobin is not photolyzed, the spectrum has been normalized to the ratio of the absorbance changes at 430 nm. The normalized reduced *minus* reduced-CO difference spectrum, which has been inverted to aid comparison with the static difference spectrum, is indicated by the solid circles (●). Panel B shows the Soret region of the postphotolysis reduced *minus* reduced-CO difference spectrum (0.2 μs) of 3.28 μM NOR in 50 mM potassium phosphate, 0.1 mM EDTA, 0.01% (w/v) DM, pH 8.0, recorded at 2.5 nm intervals (▲). The amplitude of this spectrum was normalized using the scaling factor calculated for myoglobin (panel A) and the sign changed to give a difference spectrum (---) that could be compared directly with the static reduced-CO *minus* reduced difference spectrum of NOR obtained from a sample initially reduced with dithionite (—).

Table 1

	k_{on} (M^{-1} s^{-1})[a]	ref
yeast cytochrome *c* peroxidase	2×10^3	*43*
nitric oxide synthase	2×10^4	*51*
cytochrome $P450_{cam}$ + camphor	3.7×10^4	*43*
bovine cytochrome aa_3	7×10^4	*12*
soluble guanylate cyclase	7×10^4	*52*
cytochrome caa_3 (*Bacillus subtilis*)	1.2×10^5	*53*
horse heart myoglobin	5×10^5	*43*
R−state hemoglobin (α-chains)	6.5×10^6	*43*
model heme	8.2×10^6	*43*
leghemoglobin	1.3×10^7	*43*
cytochrome *bd*	8×10^7	*44*
bacterial nitric oxide reductase	1.7×10^8	this work

[a] In multistep processes the overall apparent k_{on} is given.

CO bonds in solution are photolyzed. This makes it difficult to compare the extent of the optical changes induced by photolysis with the static reduced-CO *minus* reduced visible absorption spectrum. To overcome this difficulty, we first determined the kinetic difference spectrum immediately after photolysis of a solution of ferrous CO-bound horse myoglobin. Figure 4A shows that the postphotolysis spectrum (reduced *minus* reduced-CO) (▲) is the inverse of the static (reduced-CO *minus* reduced) difference spectrum (dashed line). However, the extent of the observed absorbance change is rather less. Comparison of the absorbance changes at 430 nm revealed a scaling factor of 1.6 that needed to be applied to the kinetic difference spectrum (●) after inversion to yield a spectrum that was essentially identical to the static difference spectrum (dashed line).

Figure 4B (▲, left *y*-axis) shows the postphotolysis (0.2 μs) difference spectrum of a sample of fully reduced, CO-bound NOR, prepared essentially as described in the legend to Figure 1A. The photolysis spectrum was normalized using the scaling factor calculated for myoglobin, assuming that the quantum yield of photolysis is similar in both enzymes. Subsequently, it was converted to molar absorption units and inverted (dashed line, right-hand *y*-axis), to facilitate comparison with the static (reduced-CO *minus* reduced) difference spectrum (dotted line, right-hand *y*-axis). The calculated kinetic difference spectrum (dashed line) is derivative-shaped with a maximum at 419 nm and a minimum at 436 nm ($\Delta\epsilon$ = 87 mM^{-1} cm^{-1}). It bears a close resemblance in form and intensity to the kinetic spectrum of myoglobin (Figure 4A). We therefore presume that after photolysis of CO, ferrous heme b_3 is both pentacoordinate and high-spin. The kinetic difference spectrum (dashed line) is clearly different in form compared with the static difference spectrum (dotted line), with a slightly red-shifted minimum (436 nm versus 433 nm) and an obvious change in the ratio of the amplitudes of the maximum and minima that is independent of the scaling factor.

Kinetics of Binding of CO to Reduced NOR. The presence of a distal sixth ligand on reduced heme b_3 may be the reason for the difference in the static and kinetic CO difference spectrum. Such a ligand is likely to influence the initial rate of CO binding to reduced NOR, a parameter that can be determined in a stopped-flow spectrometer. The rate at which CO reacts with reduced NOR (Figure 5A) is very slow compared with the rate of photolysis induced CO recombination (Figure 4). The reaction is best described by three independent exponentials (Figure 5A,B). The apparent rate constants of the two major phases were dependent on the CO concentration (Figure 5C,D). The minor third phase,

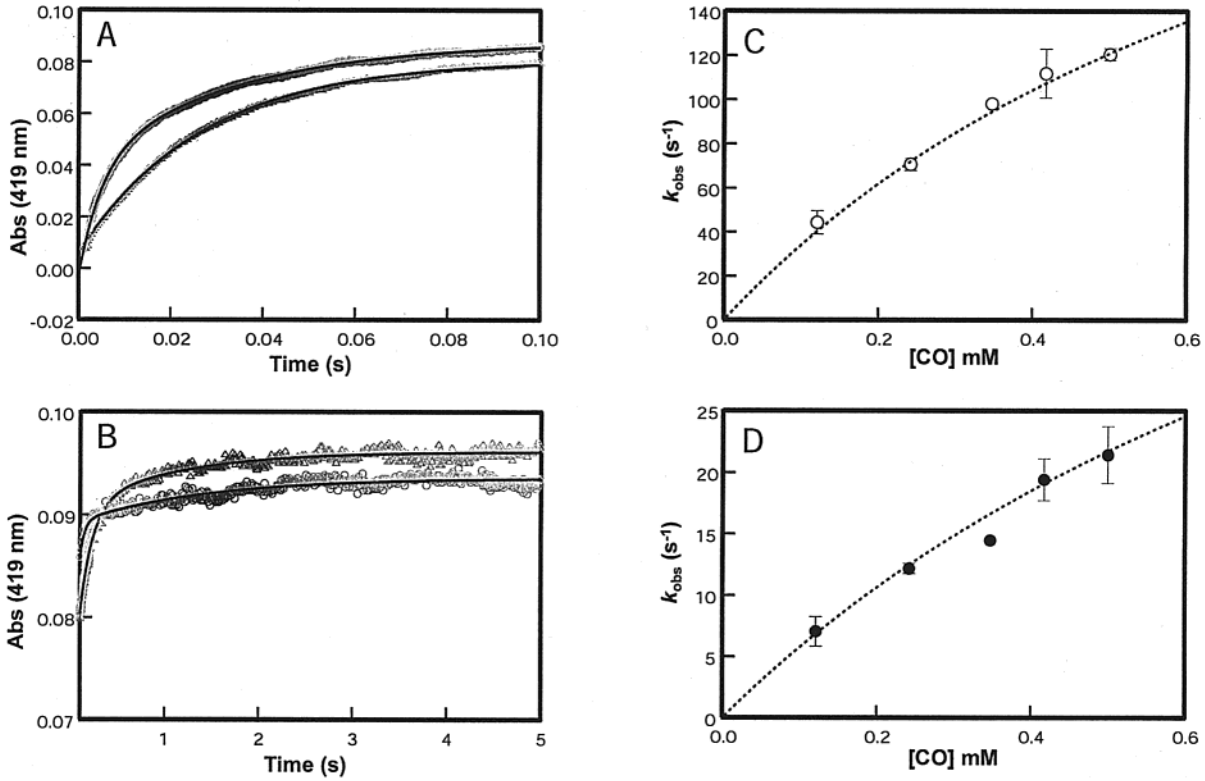

FIGURE 5: Kinetics of CO binding to reduced NOR. Panels A and B shows the experimental traces obtained from the rapid mixing of ascorbate/PMS reduced NOR (1.3 μM) with 121 μM CO (△) and 500 μM CO (○) in 25 mM TAPS, 0.01% DM, pH 8.0. The solid lines in are fits to either a single exponential or the sum of two exponentials. Panels C and D show the dependence upon CO concentration of the fast (○, panel C), and intermediate (●) phases of ligand binding (D), respectively. The error bars represent the standard deviations of the rate constants ($n = 3$). The hyperbolic lines plotted through the fast and intermediate phases represent the results of fitting of a two-step model to the data (eq 1), which used the following values: $k_{hexa} = 1.91 \times 10^5$ s^{-1} and $k_{-hexa} = 335$ s^{-1} for the fast (panel C), and $k_{hexa} = 1.48 \times 10^5$ s^{-1}, and $k_{-hexa} = 71$ s^{-1} intermediate (panel D) phases, respectively.

whose amplitude was less than 5% of the total amplitude observed, appeared independent of CO concentration and was extremely slow (<2 s^{-1}). This is attributed to reduction of any remaining Fe(III) heme b_3 by CO and subsequent formation of the Fe(II)−CO adduct.

DISCUSSION

The changes in the electronic absorption spectrum of NOR induced by CO-binding depend on both the method used to initially reduce the enzyme and the extent of reduction (Figure 1B). This is because ascorbate/PMS is unable to completely reduce the low-potential [+60 mV (*27*)] heme (heme b_3) in the active site. Incomplete reduction is indicated by the small negative feature around 600 nm in the double difference spectrum shown in Figure 1C and by the broad derivative in the Soret region of the RT-MCD spectrum (Figure 2A; solid line). The percentage of the heme b_3 remaining oxidized after reduction with ascorbate/PMS is less than 15% [estimated from the $\Delta\epsilon$ at 600 nm, using a $\Delta\epsilon$ of 7.7 mM^{-1} cm^{-1} at 600 nm for the reduction of heme b_3, calculated from the data of Grönberg et al. (*27*)]. Despite this, we preferred ascorbate/PMS to dithionite as the initial reductant for the kinetic experiments since occasionally the addition of excess dithionite to oxidized NOR led to an abnormally high Soret absorbance. The position of the Soret hardly changed upon addition of CO (not shown) and was attributed to the binding of a degradation product of dithionite to the reduced heme b_3, as has been described, e.g., for cytochrome cd_1 (*33*, *34*) and the multi-heme nitrite reductase (*35*). The presence of some residual Fe(III) heme b_3 after reduction of NOR with ascorbate/PMS is also consistent with the minor and very slow ($k_{obs} = \sim 1$ s^{-1}), concentration independent third phase in the rapid-mixing experiments.

There have been two previous reports of the static reduced-CO *minus* reduced difference spectrum of bacterial NOR (hereafter referred to simply as the CO-difference spectrum) (*22*, *23*). In both instances, the enzyme was reduced with dithionite prior to the addition of CO, and in each case, the CO-difference spectrum was different to that reported here (Figure 1B). The spectrum reported by Girsch and de Vries (*23*) shows an overall increase in absorbance at shorter wavelengths, which can be attributed to some denaturation of the protein upon addition of CO. Both the derivative-shaped feature in the Soret region, of the CO-difference spectrum, and the form and intensity in the visible region (*23*) are reminiscent of myoglobin (*36*) or cytochrome cbb_3-oxidases (*37*−*39*).

The CO-difference spectrum of NOR reported by Fujiwara and Fukumori (*22*) shows a single maximum with a shoulder in the visible region, whereas two maxima were clearly resolved in this region in the spectrum presented here (Figure 1B). The small change in the intensity of the Soret maximum reported by these authors suggests that the reduction of the enzyme was incomplete prior to the addition of CO. This is borne out by the large increase in absorbance at 563 nm and the decrease in absorbance at 615 nm that takes place when CO was added to the sample. Consequently, the CO-difference spectrum presented by these authors appears to include

a number of features that are best accounted for by further reduction of heme b_3 by CO prior to the ligand binding.

In both myoglobin and C*c*O, the kinetically determined CO-difference spectrum matches the static difference spectrum obtained after the initial binding of CO to the reduced enzyme (Figure 4A). Additionally, the rate constants for CO binding and its recombination are identical in these proteins. This implies that in these heme-proteins the binding and recombination of CO involve essentially the same processes. Comparison of the static and kinetic CO-difference spectra of NOR reveals a significant difference in the relative amplitude of the maximum compared to the minima within one spectrum (Figure 3B). Moreover, careful inspection of the minima (~400 nm) in these spectra suggests further differences. For example, in the kinetic difference spectrum, the shoulder around 400 nm shows a reduced amplitude and the minimum at 433 nm in the static spectrum appears blue-shifted to 436 nm in the kinetic difference spectrum. Moreover, the binding of CO to reduced NOR revealed two bimolecular processes with rate constants that were several orders of magnitude smaller than the recombination. Taken together, the spectroscopic and kinetic evidence suggest that CO can (re)bind to two spectroscopically different states of enzyme and that the process that is observed depends on the experimental conditions.

One explanation for the differences between the postphotolysis and static CO-difference spectra involves differences in the interaction of CO with Fe_B under the different sets of experimental conditions. However, the coordination of Fe_B is similar to the non-heme iron site of lipoxygenases (*6*), which is unable to bind CO (*40*). Given these structural considerations and an earlier FTIR experiment, which indicated that after photolysis CO only interacts transiently with Fe_B at −39 °C (*6*), any appreciable affinity of Fe_B for CO appears unlikely. Moreover, since non-heme iron shows only very weak optical changes in response to binding of diatomic ligands (<2 mM^{-1} cm^{-1}) (*41*, *42*), the significant differences between the static and postphotolysis CO difference spectra of NOR are unlikely to be due to CO binding to Fe_B.

A more plausible explanation for the differences between the initial binding of CO to Fe(II) heme b_3 and recombination is the presence of a sixth ligand on the distal face of the heme iron in part of the initially reduced enzyme, as identified in the MCD spectrum. After photolysis, CO would be expected to recombine with the pentacoordinated heme sufficiently rapidly to prevent the initially bound ligand to return prior to CO recombination. However, the need to displace this ligand will retard the rate of initial CO binding to part of the enzyme. Since a distal sixth ligand is likely to influence the optical spectrum of the reduced enzyme, this explanation can also account for the discrepancies in the kinetic and static CO-difference spectra (Figure 4A).

In presence of a sixth ligand on the reduced heme b_3, the binding of CO to reduced NOR will involve two processes: the dissociation of this sixth ligand of heme b_3, followed by the binding of CO:

$$\text{heme } b_{3,\text{HEXA}} \underset{k_{\text{HEXA}}}{\overset{k_{-\text{HEXA}}}{\rightleftharpoons}} \text{heme } b_{3,\text{PENTA}}$$

$$\text{heme } b_{3,\text{PENTA}} \underset{k_{\text{off}}}{\overset{k_{\text{on}}}{\rightleftharpoons}} \text{heme } b_3\text{-CO}$$

Since the rate constants for the dissociation of CO from ferrous heme proteins are generally less than 1 s^{-1} (*43*), we can effectively treat the second process as irreversible. Making the further assumption that binding of a sixth (distal) ligand to yield hexacoordinated heme b_3 (k_{hexa}) and the binding of CO (k_{on}[CO]) are both much faster processes than the dissociation of the sixth ligand ($k_{-\text{hexa}}$), then the observed rate constant (k_{obs}) for CO binding as a function of CO concentration can be described by eq 1.

$$k_{\text{obs}} = k_{-\text{hexA}}/(1 + k_{\text{hexA}}/k_{\text{on}}[\text{CO}]) \quad (1)$$

The flash-photolysis data indicates that the bimolecular rate constant for CO association with Fe(II) $b_{3,\text{penta}}$ is in the order of 1.7×10^8 M^{-1} s^{-1}. Using this value it was possible to successfully simulate the dependence of k_{fast} and $k_{\text{intermediate}}$ (the observed rate constants for the fast and intermediate phases of CO binding determined in the stopped flow experiments). Simulations of the dependence of both k_{fast} (Figure 5C) and $k_{\text{intermediate}}$ (Figure 5D) on CO concentration yielded a value for k_{hexa} in the range $(1.5-2) \times 10^5$ s^{-1}, a value that suggests that internal ligand rebinding might be observed in the flash photolysis experiments. However, careful inspection of our data revealed no processes that were faster than CO recombination.

It then appears that the dependence of k_{fast} and $k_{\text{intermediate}}$ on CO concentration is controlled by the rate of distal ligand debinding $k_{-\text{hexa}}$. Since the simulations show this value differs between the fast ($k_{-\text{hexa}} = 335$ s^{-1}) and intermediate ($k_{-\text{hexa}} = 71$ s^{-1}) phase we suggest that the distal ligand can exist in two forms, perhaps with different protonation states. We do not have any spectroscopic evidence that informs on the ligation state of Fe(II) heme b_3. However, we have previously demonstrated that in the three-electron reduced form of NOR, in which heme b_3 remains oxidized, that hydroxide serves as the sixth ligand.

While the presence of a sixth ligand on reduced heme b_3 could explain the relatively slow binding of CO, other properties of NOR must be responsible for the very fast rate of CO recombination. The magnitude of the bimolecular association rate constant suggests that the rate of transfer of CO from the bulk phase to heme b_3 is close to the diffusion limit, which in turn suggests that the pathway taken by CO to the active site is free of steric or electronic hindrances. This also implies that Fe_B does not influence CO recombination, as Cu_B in heme-copper oxidases does. Note that the transient interaction of CO with Fe_B after photolysis suggested by FTIR at −39 °C does not conflict with this interpretation. Observation of this complex does not imply an obligatory intermediate in the binding pathway (*44*). Additionally, the rate of CO recombination to reduced NOR may be enhanced if the proximal histidine ligand of heme b_3 has very low pK_a. Lowering the effective pK_a of a proximal histidine can enhance the rate of CO recombination up to 5-fold in the absence of other structural determinants (*8*). The relatively high frequency (1977 cm^{-1}) of the infrared stretching mode associated with the Fe−CO bond of reduced NOR (*6*), compared with heme-copper oxidases (<1965 cm^{-1}) (*45*), might also be related to such a pK_a effect.

In oxidases increasing bimolecular association rate constants for CO (Table 1) correlate with higher apparent oxygen binding rates [*bd* > *bo*$_3$ > C*c*O, see Hill et al. (*44*). Thus,

the characteristics of CO binding may be indicative for the binding rates of other diatomic gases. This suggests that these ligands use the same pathway into the binuclear center. The lack of any barrier to ligand entry into the reduced dinuclear center of NOR suggests an efficient pathway for the diffusion of substrate. This appears to be essential for the high affinity of NOR for NO, which enables this protein to maintain the steady-state concentration of NO during denitrification below toxic levels.

In the crystal structures of the aa_3-type oxidase, a large hydrophobic channel has been identified that connects the binuclear center with the membrane interface inside the cleft in subunit III (*46*, *47*). Molecular dynamics (*48*) and mutagenesis studies (*49*) have implicated this channel in oxygen transfer to the active site. The main elements of a similar pathway that may form a connection between the active site and the membrane interface appear to have been conserved in NOR, presumably to allow rapid transfer of toxic NO to the active site.

CONCLUSIONS

The reaction of reduced NOR with CO is very different from that seen in myoglobin or Cu_B-deficient oxidases. Specifically, the diffusion-limited bimolecular rate constant for CO binding to the reduced heme b_3 suggests that the pathway for diatomic gases from the bulk phase to the active site is unimpeded. This could contribute to the high affinity of NOR for NO, which would allow the enzyme to keep the intracellular NO-concentration during denitrification below toxic levels.

In part of the reduced enzyme, a barrier for the initial binding of CO exists, which is probably due to the presence of a sixth ligand on the reduced heme b_3. The need to replace this ligand is likely to interfere with NO as well as CO binding to this heme. Destabilization of the sixth ligand by NO binding to Fe_B might, however, reduce the threshold of binding to the reduced heme b_3 center for NO. A sixth ligand could be mechanistically significant in obstructing the formation of an inhibitory ferrous heme nitrosyl on heme b_3. This would be important if NO reduction occurs on Fe_B, with heme b_3 assisting the reduction by abstraction of an oxygen atom from one of the two NO molecules bound to Fe_B (*50*).

ACKNOWLEDGMENTS

We would like to thank Jeremy Thornton for his assistance in purifying the NOR used in the MCD experiments. L.P. is in receipt of a studentship from the Biomolecular Sciences Committee of EPSRC/BBSRC.

Very sadly Matti Sarate died whilst the manuscript was nearing completion. J.H.M.H., A.J.T., and N.J.W. worked closely with Matti over a number of years and are grateful to him for the opportunities that were afforded to each of us as a result of his efforts to foster collaboration between his laboratory at EMBL and the CMSB at the University of East Anglia. We hope that this publication goes some way to realizing Matti's ideal of bringing European scientists with common interests together, to further their chosen field. Thank you Matti; rest peacefully.

REFERENCES

1. Richardson, D. J., and Watmough, N. J. (1999) *Curr. Opin. Chem. Biol. 3*, 207−219.
2. Watmough, N. J., Butland, G., Cheesman, M. R., Moir, J. W. B., Richardson, D. J., and Spiro, S. (1999) *Biochim. Biophys. Acta 1411*, 456−474.
3. van der Oost, J., deBoer, A. P. N., deGier, J.-W. L., Zumft, W. G., Stouthamer, A. H., and van Spanning, R. J. M. (1994) *FEMS Microbiol. Lett. 121*, 109.
4. Castresana, J., Lübben, M., Saraste, M., and Higgins, D. G. (1994) *EMBO J. 13*, 2516−2525.
5. Cheesman, M. R., Zumft, W. G., and Thomson, A. J. (1998) *Biochemistry 37*, 3994−4000.
6. Hendriks, J., Warne, A., Gohlke, U., Haltia, T., Ludovici, C., Lubben, M., and Saraste, M. (1998) *Biochemistry 37*, 13102−13109.
7. Springer, B. A., Sligar, S. G., Olson, J. S., and Phillips, G. N. (1994) *Chem. Rev. 94*, 699−714.
8. Decatur, S. M., Franzen, S., DePillis, G. D., Dyer, R. B., Woodruff, W. H., and Boxer, S. G. (1996) *Biochemistry 35*, 4939−4944.
9. Smerdon, S. J., Krzywda, S., Wilkinson, A. J., Brantley, R. E., Carver, T. E., Hargrove, M. S., and Olson, J. S. (1993) *Biochemistry 32*, 5132−5138.
10. Shiro, Y., Iizuka, T., Marubayashi, K., Ogura, T., Kitagawa, T., Balasubramanian, S., and Boxer, S. G. (1994) *Biochemistry 33*, 14986−14992.
11. Ludwig, B., and Gibson, Q. H. (1981) *J. Biol. Chem. 256*, 92−98.
12. Gibson, Q. H., and Greenwood, C. (1963) *Biochem. J. 86*, 541−554.
13. Einarsdóttir, O., Dyer, R. B., Lemon, D. D., Killough, P. M., Hubig, S. M., Atherton, S. J., López-Garriga, J. J., Palmer, G., and Woodruff, W. H. (1993) *Biochemistry 32*, 12013−12024.
14. Lemon, D. D., Calhoun, M. W., Gennis, R. B., and Woodruff, W. H. (1993) *Biochemistry 32*, 11953−11956.
15. Alben, J. O., Moh, P. P., Fiamingo, F. G., and Altschuld, R. A. (1981) *Proc. Natl. Acad. Sci. U.S.A. 78*, 234−237.
16. Calhoun, M. W., Hill, J. J., Lemieux, L. J., Ingledew, W. J., Alben, J. O., and Gennis, R. B. (1993) *Biochemistry 32*, 11524−11529.
17. Brown, S., Rumbley, J. N., Moody, A. J., Thomas, J. W., Gennis, R. B., and Rich, P. R. (1994) *Biochim. Biophys. Acta 1183*, 521−532.
18. Mitchell, R., Moody, A. J., and Rich, P. R. (1995) *Biochemistry 34*, 7576−7585.
19. Muntyan, M. S., Ludwig, B., Zickermann, I., and Starshinova, N. P. (1998) *FEBS Lett. 429*, 216−220.
20. Verkhovsky, M. I., Morgan, J. E., and Wikström, M. (1994) *Biochemistry 33*, 3079−3086.
21. Greenwood, C., and Gibson, Q. H. (1967) *J. Biol. Chem. 242*, 1782−1787.
22. Fujiwara, T., and Fukumori, Y. (1996) *J. Bacteriol. 178*, 1866−1871.
23. Girsch, P., and de Vries, S. (1997) *Biochim. Biophys. Acta 1318*, 202−216.
24. Moënne-Loccoz, P., and de Vries, S. (1998) *J. Am. Chem. Soc. 120*, 5147−5152.
25. de Gier, J.-W. L., Lübben, M., Reijnders, W. N. M., Tipker, C. A., van Spanning, R. J. M., Stouthamer, A. H., and van der Oost, J. (1994) *Mol. Microbiol. 13*, 183−196.
26. Thomson, A. J., Cheesman, M. R., and George, S. J. (1993) *Methods Enzymol. 226*, 199−232.
27. Grönberg, K. L. C., Roldán, M. D., Prior, L., Butland, G., Cheesman, M. R., Richardson, D. J., Spiro, S., Thomson, A. J., and Watmough, N. J. (1999) *Biochemistry 38*, 13780−13786.
28. Dhawan, I. K., Shelver, D., Thorsteinsson, M. V., Roberts, G. P., and Johnson, M. K. (1999) *Biochemistry 38*, 12805−12813.
29. Burstyn, J. N., Yu, A. E., Dierks, E. A., Hawkins, B. K., and Dawson, J. H. (1995) *Biochemistry 34*, 5896−5903.
30. Bracete, A. M., Sono, M., and Dawson, J. H. (1991) *Biochim. Biophys. Acta 1080*, 264−270.
31. Vickery, L., Nozawa, T., and Sauer, K. (1976) *J. Am. Chem. Soc. 98*, 343−350.

32. Sakurai, N., and Sakurai, T. (1997) *Biochemistry 36*, 13809−13815.
33. Parr, S. R., Wilson, M. T., and Greenwood, C. (1974) *Biochem. J. 139*, 273−276.
34. Williams, P. A., Fülöp, V., Garman, E. F., Saunders, N. F., Ferguson, S. J., and Hajdu, J. (1997) *Nature 389*, 406−412.
35. Blackmore, R. S., Gadsby, P. M., Greenwood, C., and Thomson, A. J. (1990) *FEBS Lett 264*, 257−262.
36. Antonini, E., and Brunori, M. (1971) *Hemoglobin and Myoglobin in their reaction with ligands*, North-Holland Publishing Co.
37. Tamegai, H., and Fukumori, Y. (1994) *FEBS Lett 347*, 22−26.
38. Gray, K. A., Grooms, M., Myllykallio, H., Moomaw, C., Slaughter, C., and Daldal, F. (1994) *Biochemistry 33*, 3120−3127.
39. García-Horsman, J. A., Berry, E., Shapleigh, J. P., Alben, J. O., and Gennis, R. B. (1994) *Biochemistry 33*, 3113−3119.
40. Flatman, S., Hurst, J. S., McDonald-Gibson, R. G., Jonas, G. E., and Slater, T. F. (1986) *Biochim. Biophys. Acta 883*, 7−14.
41. Coufal, D. E., Tavares, P., Pereira, A. S., Hyunh, B. H., and Lippard, S. J. (1999) *Biochemistry 38*, 4504−4513.
42. Haskin, C. J., Ravi, N., Lynch, J. B., Munck, E., and Que, L., Jr. (1995) *Biochemistry 34*, 11090−11098.
43. Mims, M. P., Porras, A. G., Olson, J. S., Noble, R. W., and Peterson, J. A. (1983) *J. Biol. Chem. 258*, 14219−14232.
44. Hill, B. C., Hill, J. J., and Gennis, R. B. (1994) *Biochemistry 33*, 15110−15115.
45. Shapleigh, J. P., Hill, J. J., Alben, J. O., and Gennis, R. B. (1992) *J. Bacteriol. 174*, 2338−2343.
46. Tsukihara, T., Aoyama, H., Yamashita, E., Tomizaki, T., Yamaguchi, H., Shinzawa-Itoh, K., Nakashima, R., Yaono, R., and Yoshikawa, S. (1996) *Science 272*, 1136−1144.
47. Soulimane, T., Buse, G., Bourenkov, G. P., Bartunik, H. D., Huber, R., and Than, M. E. (2000) *EMBO J. 19*, 1766−1776.
48. Hofacker, I., and Schulten, K. (1998) *Proteins: Struct., Funct., Genet. 30*, 100−107.
49. Riistama, S., Puustinen, A., Verkhovsky, M. I., Morgan, J. E., and Wikstrom, M. (2000) *Biochemistry 39*, 6365−6372.
50. Watmough, N. J., Cheesman, M. R., Butler, C. S., Little, R. H., Greenwood, C., and Thomson, A. J. (1998) *J. Bioenerg. Biomembr. 30*, 55−62.
51. Scheele, J. S., Kharitonov, V. G., Martasek, P., Roman, L. J., Sharma, V. S., Masters, B. S., and Magde, D. (1997) *J. Biol. Chem. 272*, 12523−12528.
52. Kharitonov, V. G., Sharma, V. S., Magde, D., and Koesling, D. (1999) *Biochemistry 38*, 10699−10706.
53. Hill, B. C. (1996) *Biochemistry 35*, 6136−6143.

BI011428T